Discrete-Time, Discrete-Frequency Reassignment Method

By Daniel L. Stevens & Stephanie A. Schuckers

Clarkson University

Abstract- The reassignment method is a non-linear, postprocessin technique which cans improve the localization of a time-frequency distribution by moving its values according to a suitable vector field. The reassignment method's scheme assumes that the energy distribution in the time-frequency plane resembles a mass distribution and moves each value of the time-frequency plane located at a point (tt, ff) to another point, $(tt_\wp ff_\wp)$, which is the center of gravity of the energy distribution in the area of (tt, ff). The result is a focused representation with very high intensity [11]. During this research it was investigated and determined that the frequency reassignment corrections derived from the Flandrin reassignment method have undesired noise sensitivity at very small noise levels as well as undesired observed distortions. In order to address these issues, a novel approach was derived-the discrete-time, discrete-frequency formulation of frequency reassignment. It is shown that in noise-free tone scenarios, this novel approach eliminates ambiguity and provides less distortion than the Flandrin reassignment method.

Keywords: reassignment method, time-frequency distribution, discrete-time, discrete-frequency reassignment method.

GJRE-F Classification: FOR Code: 290901

DISCRETE-TIMEDISCRETE-FREQUENCYREASSIGNMENTMETHOD

Strictly as per the compliance and regulations of:

Discrete-Time, Discrete-Frequency Reassignment Method

Daniel L. Stevens [α] & Stephanie A. Schuckers [σ]

Abstract- The reassignment method is a non-linear, post-processing technique which cans improve the localization of a time-frequency distribution by moving its values according to a suitable vector field. The reassignment method's scheme assumes that the energy distribution in the time-frequency plane resembles a mass distribution and moves each value of the time-frequency plane located at a point (t, f) to another point, $(\hat{t}, \hat{f})$, which is the center of gravity of the energy distribution in the area of (t, f). The result is a focused representation with very high intensity [11].Duringthis research it was investigated and determined that the frequency reassignment corrections derived from the Flandrin reassignment method have undesired noise sensitivity at very small noise levels as well as undesired observed distortions. In order to address these issues, a novel approach was derived - the discrete-time, discrete-frequency formulation of frequency reassignment. It is shown that in noise-free tone scenarios, this novel approach eliminates ambiguity and provides less distortion than the Flandrin reassignment method.

Keywords: reassignment method, time-frequency distribution, discrete-time, discrete-frequency reassignment method.

I. Introduction

Bilinear time-frequency distributions offer a wide range of methods designed for the analysis of non-stationary signals. Nevertheless, a critical point of these methods is their readability [15], which means both a good concentration of the signal components along with few misleading interference terms. A lack of readability, which is a known deficiency in the classical time-frequency analysis techniques (e.g. Wigner-Ville distribution (WVD), spectrogram), must be overcome in order to obtain time-frequency distributions that can be both easily read by non-experts and easily included in a signal processing application [5]. Inability to obtain readable time-frequency distributions may lead to inaccurate signal detection and metrics extraction.

The reassignment method is a post-processing technique aimed at improving the readability of time-frequency distributions [7].The reassignment method has application to many scientific and engineering fields, including signal processing [16], biology [8], music [9], and mechanical engineering [1].The concept of time-frequency reassignment can be first traced back to Kodera in the 1970's, and was introduced in an attempt to improve the spectrogram [13].The reassignment operations proposed by Kodera could not be applied to discrete short-time Fourier transform (STFT) data, because the partial derivatives that formed these operations could not be computed directly on data that was discrete in time and frequency [6]. It has been suggested that this difficulty was a primary barrier to wider use of the reassignment method.

The next major step forward for the reassignment method was many years later when several papers were written by Auger and Flandrin [2], [4] in which reassignment equations were derived not only for the spectrogram, but also for a number of other time-frequency and time-scale distributions.

The spectrogram can be defined as a two-dimensional convolution of the WVD of the signal by the WVD of the analysis window, as in equation (1):

$$S_x(t, f; h) = \iint\limits_{-\infty}^{+\infty} W_x(s, \xi) W_h(t - s, f - \xi) ds \, d\xi \qquad (1)$$

The distribution reduces the interference terms of the signal's WVD, but at the expense of time and frequency localization. However, a closer look at equation 1 shows that $W_h(t - s, f - \xi)$ delimits a time-frequency domain at the vicinity of the (t, f) point, inside which a weighted average of the signal's WVD values is performed. The key point of the reassignment principle is that these values have no reason to be symmetrically distributed around (t, f), which is the geometrical center of this domain. Therefore, their average should not be assigned at this point, but rather at the center of gravity of this domain, which is much more representative of the local energy distribution of the signal [3]. Reasoning with a mechanical analogy, the local energy distribution $W_h(t - s, f - \xi) W_x(s, \xi)$ (as a function of s and ξ) can be considered as a mass distribution, and it is much more accurate to assign the total mass (i.e. the spectrogram value) to the center of gravity of the domain rather than to its geometrical center. Another way to look at it is this: the total mass of an object is assigned to its geometrical center, an arbitrary point

Author α: Air Force Research Laboratory Rome, NY 13441.
e-mail: daniel.stevens.7@us.af.mil
Author σ: Department of Electrical and Computer Engineering, Clarkson University. Potsdam, NY 13699.
e-mail: sschucke@clarkson.edu

which except in the very specific case of a homogeneous distribution, has no reason to suit the actual distribution. A much more meaningful choice is to assign the total mass of an object, as well as the spectrogram value, to the center of gravity of their respective distribution [5].

This is exactly how the reassignment method proceeds: it moves each value of the spectrogram computed at any point (t, f) to another point $(\hat{t}, \hat{f})$ which is the center of gravity of the signal energy distribution around (t, f)[12](see equations (2) and (3)):

$$\hat{t}(x; t, f) = \frac{\iint_{-\infty}^{+\infty} s\, W_h(t - s, f - \xi)W_x(s, \xi)ds\, d\xi}{\iint_{-\infty}^{+\infty} W_h(t - s, f - \xi)W_x(s, \xi)ds\, d\xi} \tag{2}$$

$$\hat{f}(x; t, f) = \frac{\iint_{-\infty}^{+\infty} \xi\, W_h(t - s, f - \xi)W_x(s, \xi)ds\, d\xi}{\iint_{-\infty}^{+\infty} W_h(t - s, f - \xi)W_x(s, \xi)ds\, d\xi} \tag{3}$$

and thus leads to a reassigned spectrogram (equation (4)), whose value at any point (t', f') is the sum of all the spectrogram values reassigned to this point:

$$S_x^{(r)}(t', f'; h) = \iint\limits_{-\infty}^{+\infty} S_x(t, f; h)\delta(t' - \hat{t}(x; t, f))\delta\left(f' - \hat{f}(x; t, f)\right) dt\, df \tag{4}$$

One of the most interesting properties of this new distribution is that it also uses the phase information of the STFT, and not only its squared modulus as in the spectrogram. It uses this information from the phase spectrum to sharpen the amplitude estimates in time and frequency. This can be seen from the following expressions of the reassignment operators:

$$\hat{t}(x; t, f) = -\frac{d\Phi_x(t, f; h)}{df} \tag{5}$$

$$\hat{f}(x; t, f) = f + \frac{d\Phi_x(t, f; h)}{dt} \tag{6}$$

Where $\Phi_x(t, f; h)$ is the phase of the STFT of x : $\Phi_x(t, f; h) = \arg\ F_x(t,\quad f;\quad h))$. However, these expressions (equations (5) and (6)) do not lead to an efficient implementation, and have to be replaced by equations (7) (local group delay) and (8) (local instantaneous frequency):

$$\hat{t}(x; t, f) = t - \Re\left\{\frac{F_x(t, f; T_h)F_x^*(t, f; h)}{|F_{x(t\,f;h}|^2}\right\} \tag{7}$$

$$\hat{f}(x; t, f) = f - \Im\left\{\frac{F_x(t, f; D_h)F_x^*(t, f; h)}{|F_{x(t, f; h}|^2}\right\} \tag{8}$$

Where $T_h(t) = t \times h(t)$ and $D_h(t) = \frac{dh}{dt}(t)$. This leads to an efficient implementation for the reassigned spectrogram without explicitly computing the partial derivatives of phase. The reassigned spectrogram may thus be computed by using 3 STFTs, each having a different window (the window function h; the same window with a weighted time ramp t*h; the derivative of the window function h with respect to time (dh/dt), (also known as the frequency-weighted window)).

Reassigned spectrograms are therefore very easy to implement, and do not require a drastic increase in computational complexity.

Since time-frequency reassignment is not a bilinear operation, it does not permit a stable reconstruction of the signal. In addition, once the phase information has been used to reassign the amplitude coefficients, it is no longer available for use in reconstruction. This is perhaps why the reassignment method has received limited attention from engineers, and why its greatest potential may be where reconstruction is not necessary, that is, where signal analysis is an end unto itself.

The reassignment principle for the spectrogram allows for a straight-forward extension of its use to other distributions as well [10]. If we consider the general expression of a distribution of the Cohen's class as a two-dimensional convolution of the WVD, as in equation (9):

$$C_x(t, f; \Pi) = \iint\limits_{-\infty}^{+\infty} \Pi(t - s, f - \xi)W_x(s, \xi)ds\, d\xi \tag{9}$$

replacing the particular smoothing kernel $W_h(u, \xi)$ by an arbitrary kernel $\Pi(s, \xi)$ simply defines the reassignment of any member of Cohen's class (equations (10) through (12)):

$$\hat{t}(x; t, f) = \frac{\iint_{-\infty}^{+\infty} s\, \Pi(t - s, f - \xi)W_x(s, \xi)ds\, d\xi}{\iint_{-\infty}^{+\infty} \Pi(t - s, f - \xi)W_x(s, \xi)ds\, d\xi} \tag{10}$$

$$\hat{f}(x; t, f) = \frac{\iint_{-\infty}^{+\infty} \xi\, \Pi(t - s, f - \xi)W_x(s, \xi)ds\, d\xi}{\iint_{-\infty}^{+\infty} \Pi(t - s, f - \xi)W_x(s, \xi)ds\, d\xi} \tag{11}$$

$$C_x^{(r)}(t', f'; \Pi) = \iint\limits_{-\infty}^{+\infty} C_x(t, f; \Pi)\delta(t' - \hat{t}(x; t, f))\delta\left(f' - \hat{f}(x; t, f)\right) dt\, df \tag{12}$$

The resulting reassigned distributions efficiently combine a reduction of the interference terms provided by a well adapted smoothing kernel and an increased concentration of the signal components achieved by the reassignment. In addition, the reassignment operators $\hat{t}(x; t, f)$ and $\hat{f}(x; t, f)$ are almost as easy to compute as for the spectrogram [4].

Similarly, the reassignment method can also be applied to the time-scale energy distributions [14]. Starting from the general expression in equation (13):

$$\Omega_x(t, a; \Pi) = \iint_{-\infty}^{+\infty} \Pi(s/a, f_0 - a\xi) W_x(t - s, \xi) \, ds \, d\xi \tag{13}$$

we can see that the representation value at any point $(t, a = f_0/f)$ is the average of the weighted WVD values on the points $(t - s, \xi)$ located in a domain centered on (t, f) and bounded by the essential support of Π. In order to avoid the resultant signal components

broadening while preserving the cross-terms attenuation, it seems once again appropriate to assign this average to the center of gravity of these energy measures, whose coordinates are shown in equations (14) and (15):

$$\hat{t}(x; t, f) = t - \frac{\iint_{-\infty}^{+\infty} s \, \Pi(s/a, f_0 - a\xi) W_x(t - s, \xi) ds \, d\xi}{\iint_{-\infty}^{+\infty} \Pi(s/a, f_0 - a\xi) W_x(t - s, \xi) ds \, d\xi} \tag{14}$$

$$\hat{f}(x; t, f) = \frac{f_0}{\hat{a}(x; t, f)} = \frac{\iint_{-\infty}^{+\infty} \xi \, \Pi(s/a, f_0 - a\xi) W_x(t - s, \xi) ds \, d\xi}{\iint_{-\infty}^{+\infty} \Pi(s/a, f_0 - a\xi) W_x(t - s, \xi) ds \, d\xi} \tag{15}$$

Rather than to the point $(t, a = f_0/f)$ where it is computed. The value of the resulting modified time-scale representation on any point (t', a') is then the sum of all the representation values moved to this point, and is known as the reassigned scalogram (equation (16)):

It can be shown that the reassignment method is theoretically perfectly localized for chirps and impulses.

Fig. 1 clearly shows the improvement in readability that the reassignment method provides over its classical time-frequency distribution counterpart. This is due to the reassignment method's 'smoothing' and 'squeezing' qualities.
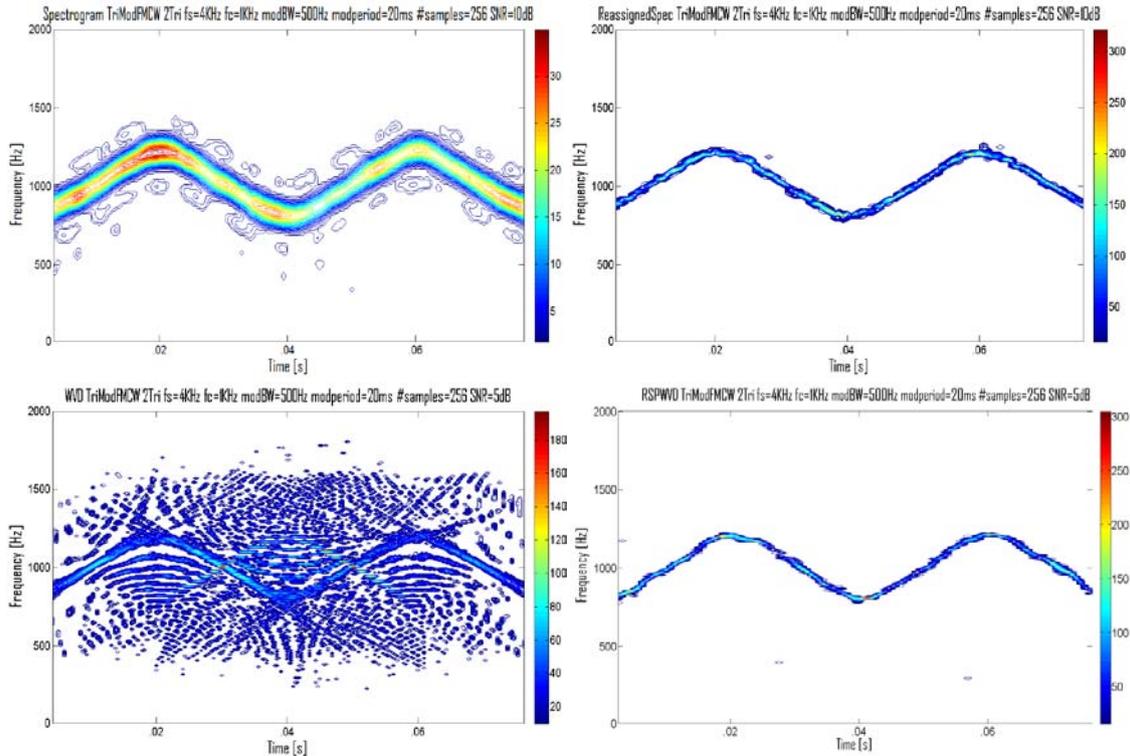

Figure 1: Time-frequency localization comparison between the classical time-frequency analysis tools (left) and the reassignment method (right). The upper two plots are the spectrogram (left) and the reassigned spectrogram (right) for a triangular modulated FMCW signal (256 samples, SNR=10dB), and the lower two plots are the WVD

(left) and the reassigned smoothed-pseudo WVD (RSPWVD) (right) for a triangular modulated FMCW signal (256 samples, SNR=5dB). The reassignment method gives a much more concentrated time-frequency localization, and produces a reduction in cross-term interference, which makes for an improvement in readability over its classical time-frequency distribution counterpart [17].

Table I supports the hypothesis that the improved readability provided by the reassignment method (shown in Fig. 1) translates to more accurate signal detection and parameter metrics extraction.

Table I: Test metrics comparison between the spectrogram and the reassigned spectrogram and between the WVD and the RSPWVD (> 600 total test runs) [17]
('*' denotes outperformed its counterpart; '~' denotes performed about equal to its counterpart)

Parameters Extracted	Spectrogram	Reassigned Spectrogram	WVD	RSPWVD
Carrier Frequency (% error)	~ 1.0%	~ 1.9%	~ 2.5%	~ 3.4%
Modulation Bandwidth (% error)	22.2%	* 1.0%	6.8%	* 3.9%
Modulation Period (% error)	~ 0.5%	~ 0.4%	~ 0.3%	~ 0.2%
TF Localization (X) (% of entire x-axis)	3.0%	* 1.1%	~ 0.65%	~ 0.69%
TF Localization (Y) (% of entire y-axis)	7.1%	* 2.2%	~ 1.54%	~ 1.48%
Chirp Rate (% error)	21.7%	* 0.6%	6.6%	* 4.6%
Percent Detection (0,10dB)	93.0%	* 100%	89.3%	* 95.0%
Lowest Detectable SNR	*-3.5 dB	-2.5 dB	-2.0 dB	*-3.0 dB
Plot Time	* 4.0 s	33.0 s	12m:54s	* 34.9 s

Experimental tests and analyses of the reassignment method algorithms in MATLAB (such as those illustrated above) have demonstrated the effectiveness of the reassignment method. Using simple threshold detection methods, visual inspection of a variety of input reassigned signals and detection results led to the conclusion that these results corresponded quite well with human assessment of the reassigned signals.

II. Concerns Discovered with the Flandrin Frequency Reassignment Method

While performing research under this effort for the purpose of obtaining quantitative performance measures for the reassignment method, it was discovered that the frequency reassignment corrections derived from the Flandrinre assignment method had undesired noise sensitivity at very small noise levels as well as undesired observed distortions.

The equation for the standard reassignment method is shown in equation (17):

$$frequency\ reassignment\ correction = \frac{-N}{2\pi} \cdot Im\left\{\frac{X_{hD}[n,k]}{X_h[n,k]}\right\} \tag{17}$$

This value is added to the frequency bin (index k), to correct for frequency assignment. Here, N is the DFT length (and signal segment length when no zero-padding is used). $X_h[n,k]$ is a DFT of the weighted input, formed from an N-length segment of the input x[n], multiplied by the N-length window, h[n]. $X_{hD}[n,k]$ is the DFT of the same input segment, but in this case, weighted (multiplied) by the "derivative" of the data window. The indices n and k are the time (sample) index and the frequency (bin) index respectively.

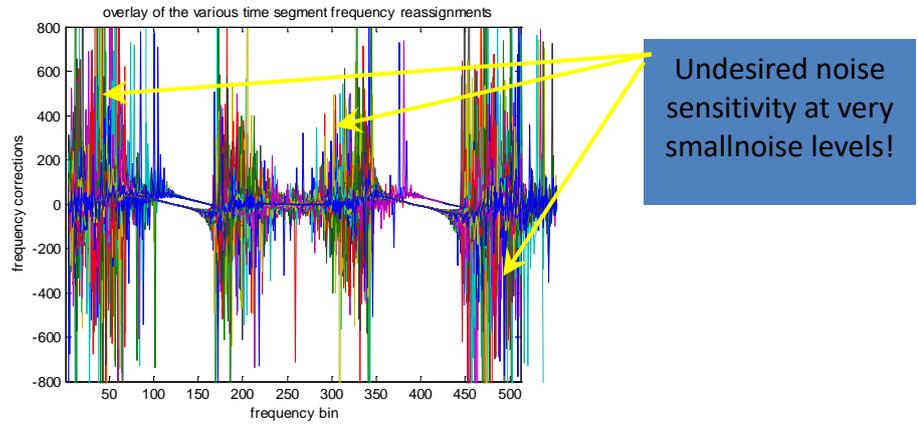Figure 2 shows the undesired noise sensitivity at very small noise levels using Flandrin's reassignment method.

Figure 2: Frequency reassignment corrections derived from Flandrin et. al. algorithm. SNR=97dB and tone is located near bin 121. Undesired noise sensitivity is observed at very small noise levels.

Figure 3 is a plot of frequency bin vs. frequency corrections, again using the Flandrin frequency reassignment corrections algorithm (equation (17)), but this time with noise-free tones located near bin 0. The plot shows undesired observed distortions in noise-free frequency reassignment, as well as multi-valued corrections, implying ambiguity, and making uniquely correcting for distortions impossible.
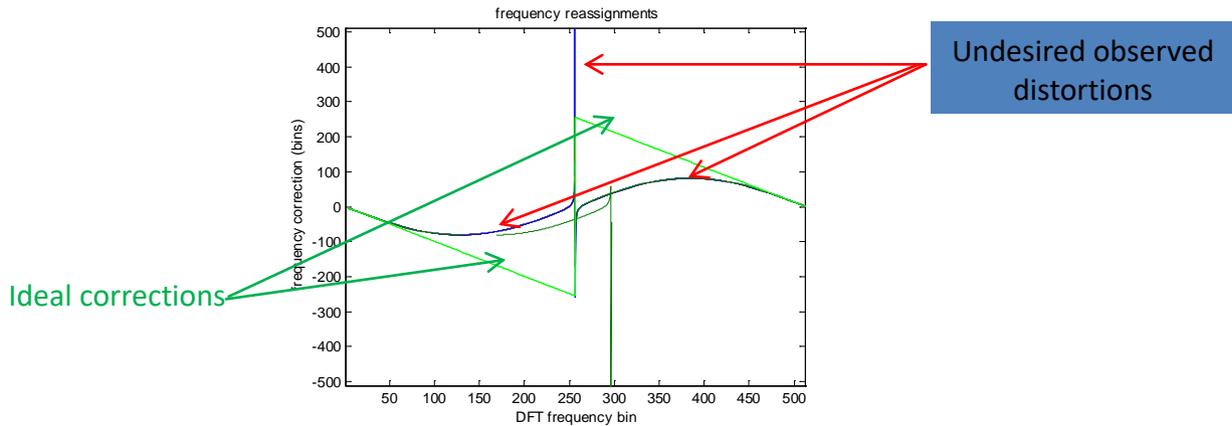

Figure 3: Frequency reassignment corrections derived from Flandrin et. al. algorithm. Noise-free tones located near bin 0. Plot shows distortions in noise-free frequency reassignment.

III. INCEPTION OF THE DISCRETE-TIME, DISCRETE-FREQUENCY (D&D) REASSIGNMENT METHOD

Analyzing the frequency reassignments for the DFT of such a weighted data segment we can omit for now the time reassignment, which allows simplification of equation (17) as,

$$R[k] = \frac{-N}{2\pi} \cdot Im\left\{\frac{X_{hD}[k]}{X_h[k]}\right\} \qquad (18)$$

or equivalently

$$R[k] = Im\left\{\frac{-N}{2\pi} \cdot W[k]\right\} \qquad (19)$$

With

$$W[k] = \frac{X_{hD}[k]}{X_h[k]} \qquad (20)$$

The sequence domain multiplication from the application of the data window results in circular convolution in the frequency domain, which allows us to write

$$\frac{X_{hD}[k]}{X_h[k]} = \frac{X[k] \circledast H_D[k]}{X[k] \circledast H[k]} \qquad (21)$$

In the continuous-time, continuous-frequency original formulation of the frequency reassignment process, the weighting function, $h'(t)$, is the time-derivative of $h(t)$.

However, this relationship is a result of linear convolutional processes that occur in the domains of continuous-time and continuous-frequency.

For the discrete-time, discrete-frequency (D&D) formulation of frequency reassignment, we need to account for the circular convolutions as identified in equation (21).

Accounting for circular convolution allows us to determine the relationship between

$$h[n] = DFT^{-1}\{H[k]\} \qquad (22)$$

and

$$h_D[n] = DFT^{-1}\{H_D[k]\} \qquad (23)$$

We first return to the goal of frequency reassignment, which is to eliminate the spreading of sinusoidal components in the frequency representation of $x_h[n]$ as observed in the transform result, $X_h[k]$(i.e. we want localization in frequency).

This tells us that the desired result of Equation (19) is a (modulo-N for complex-valued inputs) ramp sequence, such that an input sinusoid is reassigned to a single frequency bin.

If we impose the requirement that the calculation in Equation (20) is purely imaginary valued for a given input sinusoid, likewise, $W[k]$can be determined from Equation (19).

With $W[k]$ known for an input complex exponential sinusoid, $x_{cs}[n]$, from Equations (20) and (21), we can solve for $h_D[n]$ in terms of $h[n]$, which results in

$$h_D[n] = \frac{DFT^{-1}\{W[k] \cdot DFT\{h[n] \cdot x_{cs}[n]\}\}}{x_{cs}[n]} \qquad (24)$$

Note that the above Equation (24) represents a pre-processing step that can be performed as an initialization for determining$h_D[n]$, for a chosen data window,$h[n]$. Equation (24) represents the first iteration of the D&D reassignment method.

For any arbitrary input,$x[n]$, these data windows can be considered for use as implied in Equation (19) to accomplish the frequency reassignments.

As a practical matter, caution must be used to ensure that the denominator in Equation (24) does not result in division by zero.

A logical choice for the complex sinusoid, $x_{cs}[n]$, is one that maximally spreads energy across frequency bins, i.e., one that is at a frequency that lies exactly between two bin centers (i.e. choose the worst-case scenario for localization).

In this sense, the chosen sinusoid is a design signal, which allows us to elicit a response from the system of Equation (24), which is used as our "time-derivative" data window.

Observations made by following this method exposes the sensitivity of Equation (17) to the selection of an appropriate derivative of the data window, as can be seen in figure 4.
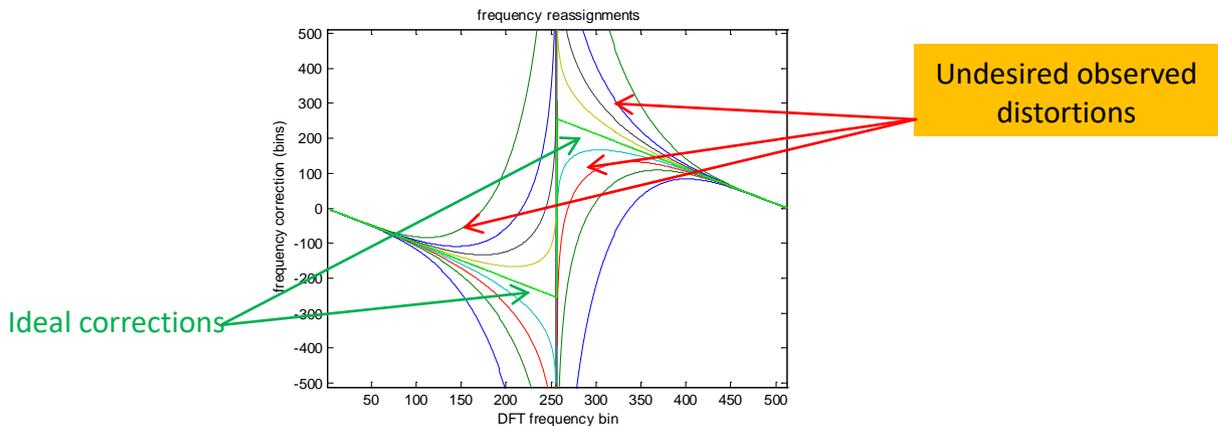
Figure 4: Frequency reassignment corrections derived from above method. Nine noise-free tones located near bin 0. Plot shows undesired observed distortions and that the response is observed to be highly sensitive to the input signal frequency, and implicitly to the determination of derivative of window, h. Note that when he input signal matches the design signal, ideal reassignment is achieved.

IV. Further Enhancement of the D&D Reassignment Method

In an attempt to resolve some of the issues noted in figure 4, frequency reassignment corrections were derived from exact mathematical derivative (i.e. Hanning, derivative of Hanning), followed by sampling. Figure 5 shows the results of this approach.
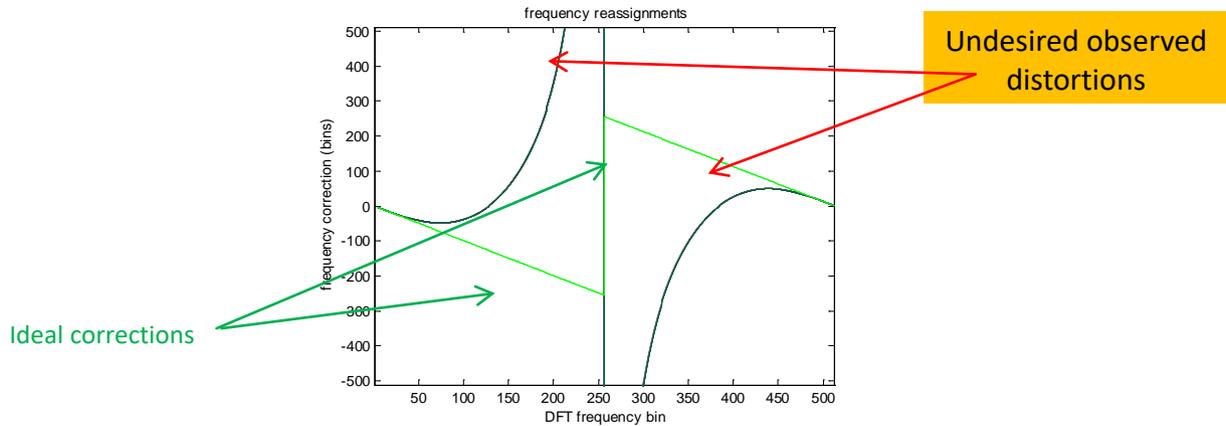
6

Figure 5: Frequency reassignment corrections derived from exact mathematical derivative (i.e. Hanning, derivative of Hanning), followed by sampling. Nine noise-free tones located near bin 0. The plot shows some improvement over figure 4 (consistent), but still has issues (undesired observed distortions, creates excessive distortion, is multi-valued causing ambiguity).

Continuing in an attempt to resolve issues brought out in figure 4 and figure 5, frequency reassignment corrections were derived from DFT-based scaling by jw as a derivative approximation (represents the most current state of development of the D&D reassignment method). Figure 6 shows the promising results of this approach.
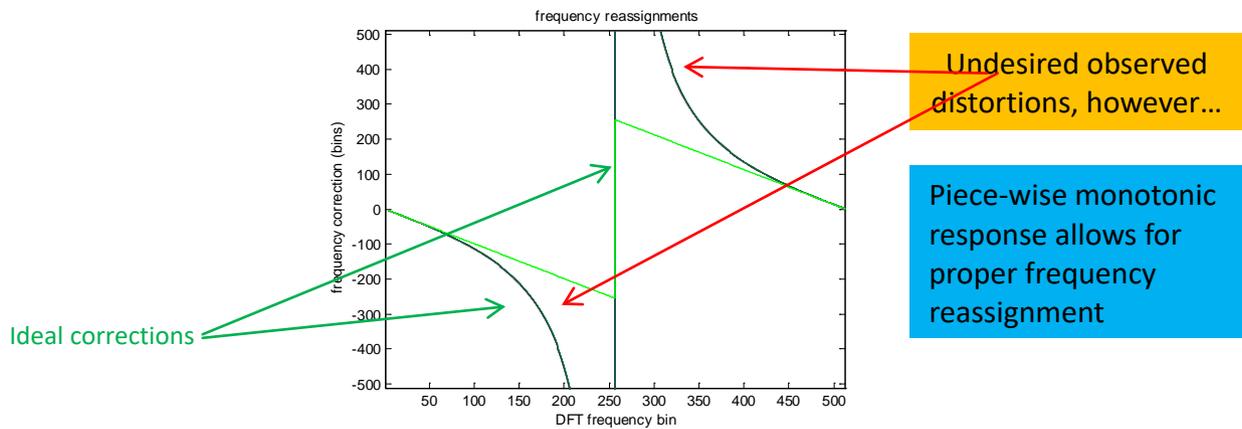

Figure 6: Frequency reassignment corrections derived from DFT-based scaling by jw as a derivative approximation (most current state of development of the D&D reassignment method). Nine noise-free tones located near bin 0. There are undesired observed distortions, however, using piece-wise monotonic response will allow for proper frequency reassignment. Eliminates the ambiguity, is consistent, with less distortion than prior methods. Shows a marked improvement over the methods used to produce figure 4 and figure 5. This most current state of development of the D&D reassignment method will be used to compare reassignment results to Flandrin's method.

Figure 7 shows comparisons of the original spectrogram, the Flandrin frequency reassignment, and the D&D frequency reassignment derived from DFT-based scaling by jw as a derivative approximation (noise-free tone (top row) and 80dB SNR (bottom row)). For the noise-free tone (top row), the D&D frequency reassignment clearly produces better results. For the bottom row, the blue band around the yellow line is more narrow (meaning more of the energy is reassigned) for the D&D frequency reassignment than for the Flandrin frequency reassignment (figure 8 substantiates this).

Original Spectrogram

Frequency Reassignment (baseline – Flandrin)

Frequency Reassignment (D&D – most current)

Figure 7: Comparisons of original spectrogram (left), baseline (Flandrin) frequency reassignment (center), and most current D&D frequency reassignment (right). The top row is for a noise-free tone, and the bottom row is for 80dB SNR. For the noise-free tone (top row), the D&D frequency reassignment clearly produces better results. For the bottom row, the blue band around the yellow line is more narrow (meaning more of the energy is reassigned) for the D&D frequency reassignment than for the Flandrin frequency reassignment (figure 8 substantiates this).
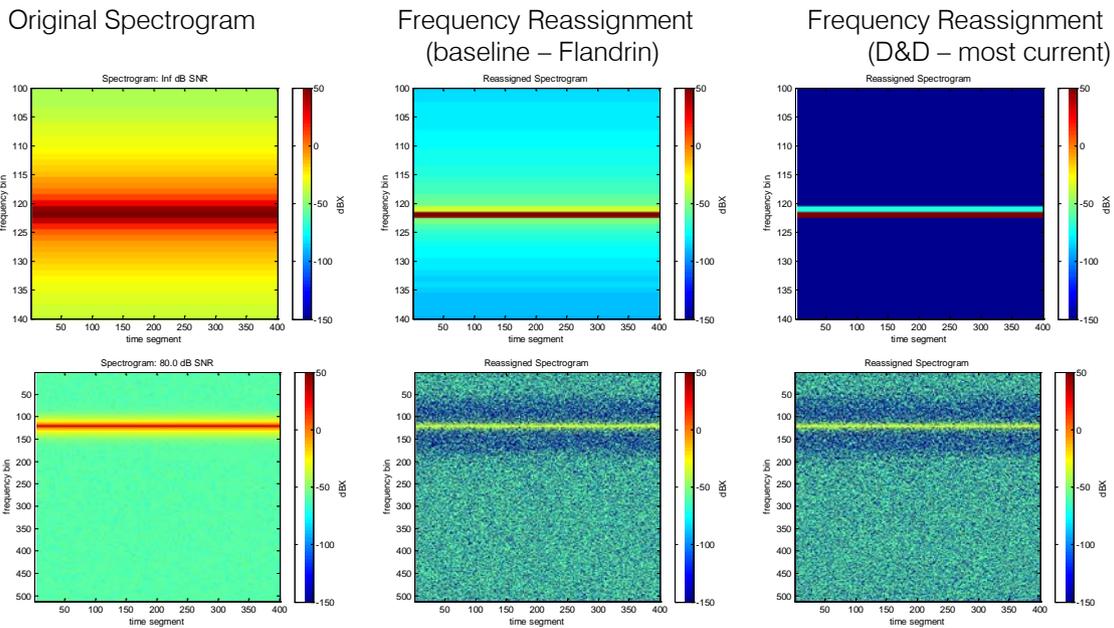
Figure 8, which represents new work in the area of preliminary statistical investigation, is a time accumulation comparison (similar to a Hough Transform) between Flandrin's frequency reassignment at 80dB SNR and the D&D frequency reassignment derived from DFT-based scaling by jw as a derivative approximation at 80dB SNR. Though the processing gain is evident for Flandrin's frequency reassignment, the processing gain is even more enhanced for the D&D frequency reassignment, showing both an increase in strength of the reassigned tone and a decrease in noise floor, leading to an improvement in detect ability at a commensurate false alarm rate. This substantiates the findings of figure 7 that more of the energy is reassigned in the bottom right plot (D&D) than in the bottom center plot (Flandrin).
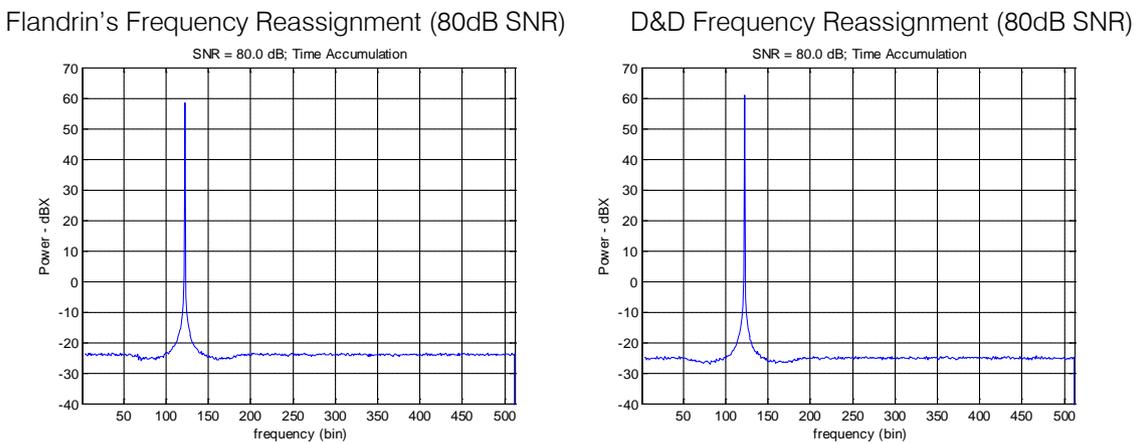
Flandrin's Frequency Reassignment (80dB SNR)

D&D Frequency Reassignment (80dB SNR)

Figure 8: Time accumulation (i.e. representative of Hough Transform) comparison of baseline (Flandrin) frequency reassignment (left), and the most current D&D frequency reassignment (right) (both at 80dB SNR).Though processing gain is evident for Flandrin frequency reassignment, processing gain is even more enhanced for the D&D frequency reassignment, which shows both an increase in strength of reassigned tone and a decrease in noise floor, leading to an improvement in detectability at a commensurate false-alarm rate.

V. Conclusions

During this research it was investigated and determined that the frequency reassignment corrections derived from the Flandrin reassignment method have undesired noise sensitivity at very small noise levels as well as undesired observed distortions. To address these issues, the novel approach of the discrete-time, discrete-frequency (D&D) formulation of frequency reassignment was derived. It is shown that in noise-free tone scenarios, this novel approach (the D&D reassignment method) eliminates ambiguity and provides less distortion than the Flandrin reassignment method.

As a result of the derivation and enhancement of the D&D reassignment method, one of the focus areas for future research efforts will be a comparison between the D&D reassignment method and the standard (Flandrin's) reassignment method for not only frequency reassignment corrections, but also for time reassignment corrections, in both noise-free and high noise (low SNR) environments. Also, investigation will be performed using the D&D reassignment method to further reduce undesired observed distortions for both noise-free and high noise (low SNR) environments. Publishing and patent efforts have come about as a result of this research [18], and will continue as the research develops.

References Références Referencias

1. Aime, J., Brissaud, M., Laguerre, L., Generation and Detection of Elastic Guided Waves with Magneto elastic Device for the Nondestructive Evaluation of Steel Cables and Bars. In Proc. 15th World Conference on Nondestructive Testing, Rome, Italy, 2000.
2. Auger, F., Flandrin, P., Generalization of the Reassignment Method to all Bilinear Time-Frequency and Time-Scale Representations. In Proc. ICASSP, Volume IV, pages 317-20, 1994.
3. Auger, F., Flandrin, P., the Why and How of Time-Frequency Reassignment. IEEE International Symposium on Time-Frequency and Time-Scale Analysis, pp. 197-200, 1994.
4. Auger, F., Flandrin, P., Improving the Readability of Time-Frequency and Time-Scale Representation by the Reassignment Method. IEEE Transactions on Signal Processing, 43(5):1068-1089, 1995.
5. Boashash, B., Time Frequency Signal Analysis and Processing: A Comprehensive Reference. Elsevier, Oxford, England, 2003.
6. Fitz, K., Fulop, S., A Unified Theory of Time-Frequency Reassignment. Digital Signal Processing, September 30, 2005.
7. Flandrin, P., Auger, F., Chassande-Mottin, E., Time-Frequency Reassignment: From Principles to Algorithms. CRC Press LLC, 2003.
8. Gardner, T., Magnasco, M., Sparse Time-Frequency Representations. Proceedings for the National Academy of Sciences, Vol. 103, No. 16, pp. 6094-6099, April 18, 2006.
9. Hainsworth, S., Macleod, M., Time Frequency Reassignment: A Review and Analysis. Technical Report, Cambridge University Engineering Dept., Cued/F-Infeng/TR.459.
10. Hippenstiel, R., Fargues, M., Moraitakis, I., Williams, C., Detection and Parameter Estimation ofChirped Radar Signals. Final Report, Naval Postgraduate School, Monterey, A, Jan. 10, 2000.
11. Lemoine, O., Auger, F., Flandrin, P., Goncalves, P., Time-Frequency Toolbox Users Manual. CentreNational de la Recherche Scientifique and Rice University, 1996.
12. Li, X., Bi, G., A New Reassigned Time-Frequency Representation. 16th European Signal Processing Conference, Lausanne, Switzerland, pp. 1-4, August 25-29, 2008.
13. Ozdemir, A., Time-Frequency Component Analyzer. Dissertation, Bilkent University, Ankara,Turkey,Sept. 2003.
14. Rioul, O., Flandrin, P., Time-Scale Energy Distributions: A General Class Extending Wavelet Transforms. IEEE Transactions on Signal Processing, Vol. SP-40, No. 7, pp. 1746-1757, 1992.
15. Stephens, J., Advances in Signal Processing Technology for Electronic Warfare. IEEE AES Systems Magazine, pp. 31-38, November 1996.
16. Stevens, D., Detection and Parameter Extraction of Low Probability of Intercept Radar Signals Using the Reassignment Method and the Hough Transform. Dissertation, Clarkson University, Potsdam, NY, 2010.
17. Stevens, D., Schuckers, S., Detection and Parameter Extraction of Triangular Modulated FMCW LPI Radar Signals Using the Reassignment Method. 2nd Annual AOC Symposium on Low Probability of Intercept Radar & Counter-LPI Technology, Naval Postgraduate School, Monterey, CA, pp. 1-4, February 15-17, 2011
18. A. Noga, D. Stevens, "Apparatus for Frequency Measurement," U.S. Patent 9,778,298; 03 October 2017.